Proc. Lunar Sci. Conf. 6th (1975), p. 2721–2738.
Printed in the United States of America

Photogeological, geophysical, and geochemical data on the east side of the moon

FAROUK EL-BAZ

National Air and Space Museum, Smithsonian Institution, Washington, D.C. 20560

D. E. WILHELMS

U.S. Geological Survey, Menlo Park, California 94025

Abstract—Correlations were made between Apollo orbital data and geologic data from eight map provinces in a region centered on the east limb of the moon (50°N to 50°S and 50°E to 140°E). The provinces include old and young dark-colored plains (volcanic basalts), and old and young light-colored plains of impact and/or volcanic origin. Four more rugged terra provinces are rugged young basin rim materials, lineated basin ejecta, tracts of terra that appear to be mantled, and a province of densely cratered primitive terra.

Laser altimeter measurements, which are used to make geologic cross sections, indicate that the western (nearside) part of the region averages about 3 km lower in elevation than the eastern (farside) part. Gravity data correlate with most geologic provinces and the surface profiles made by the laser altimeter and lunar sounder. Most positive gravity anomalies correlate with deep, mare-filled basins, and negative anomalies correlate with relatively shallow, light-plains-filled basins and craters.

The X-ray fluorescence experiment shows extreme values of concentration ratios of Al:Si and Mg:Si over large areas where a single geologic province predominates. These ratios are in general inversely related, e.g. the mare-free cratered terra province has the two highest Al:Si and the two lowest Mg:Si ratios. The inverse relation holds over the maria—low-Al:Si and high-Mg:Si ratios—except where materials may be mixed. Gamma-ray spectrometry indicates that most of the region has relatively low natural radioactivity. The highest, but still moderate, readings are over the maria and a plains province east of Langrenus. These and other correlations with orbital data add to the understanding of the geologic history of the studied region.

INTRODUCTION

MOST OF THE LUNAR NEAR SIDE has been geologically mapped at 1:5,000,000 scale (Wilhelms and McCauley, 1971). To complete the geologic mapping of the moon, the remaining part was divided into five regions: the east side, west side, central far side, and north and south sides. We have collaborated in studying the east side of the moon and the resulting geologic map is in press (Wilhelms and El-Baz, 1976).

The region named the east side of the moon is centered on the east limb, and lies between 50°N and 50°S latitudes and 50°E and 140°E longitudes (Fig. 1). In this region, which encompasses about 8,000,000 km^2, maria are concentrated on the western or nearside part and terrae or highlands dominate the eastern or farside part (Fig. 2).

Detailed geologic study of the region was based on all available Lunar Orbiter images and Apollo photographs. The Apollo 15, 16, and 17 metric and panoramic orbital photographs were particularly useful, even though their coverage was

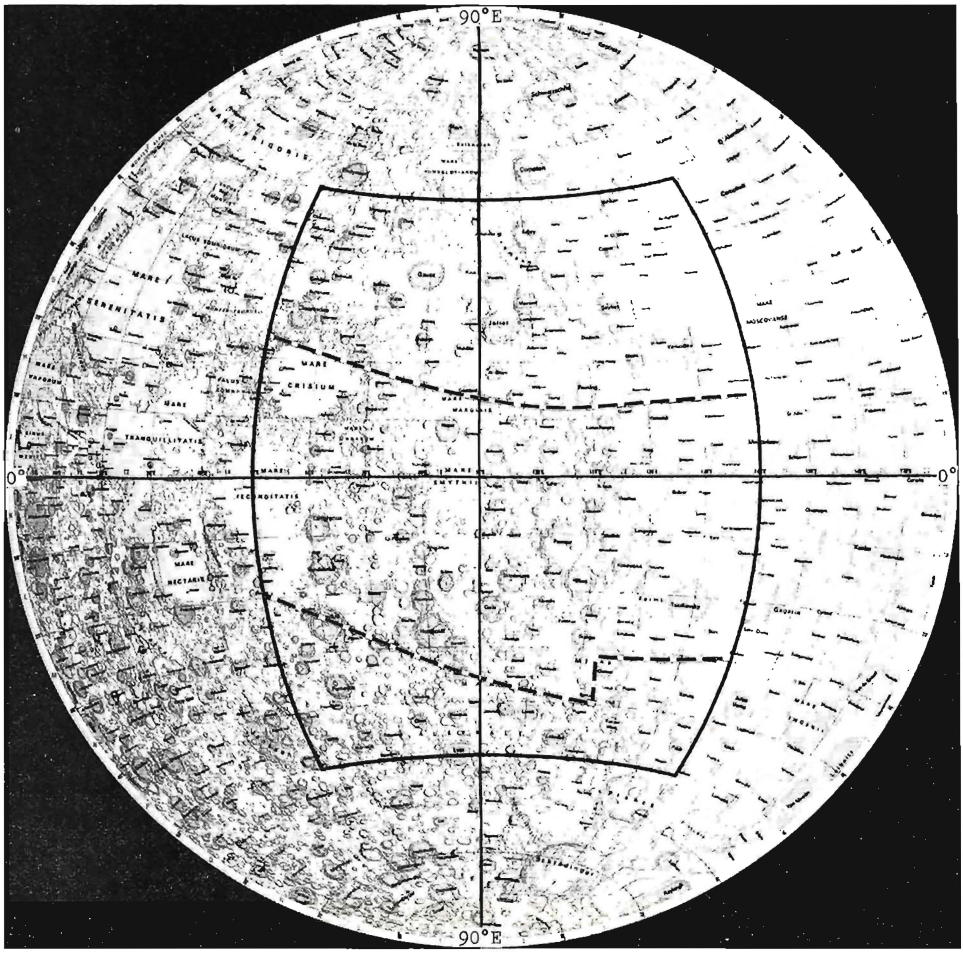

Fig. 1. The mapped east side region of the moon outlined on a map of the lunar eastern hemisphere by Rükl (1972). The region is centered on the east limb between latitude 50°N and 50°S, and longitude 50°E and 140°E. Dashed lines indicate the coverage of stereo photographs taken from orbit by metric cameras on Apollo missions 15, 16, and 17. North and south of these dashed lines the region is covered by Lunar Orbiter images, and partly by metric and panoramic Apollo pictures taken during trans-earth coast.

limited to an equatorial band (Fig. 1). Photographs from both camera systems taken after trans-earth injection covered, at lower resolution, most of the region (see example in Fig. 2).

In the course of geologic mapping, it became obvious that data obtained by sensors other than cameras may aid in understanding the features portrayed in photographs. Geophysical and geochemical sensors flown in the orbiting Command/Service Module on Apollo mission 15, 16, and 17 provided voluminous data pertaining to the region. This paper is an attempt to correlate photogeologic interpretations and some of these remotely sensed data.

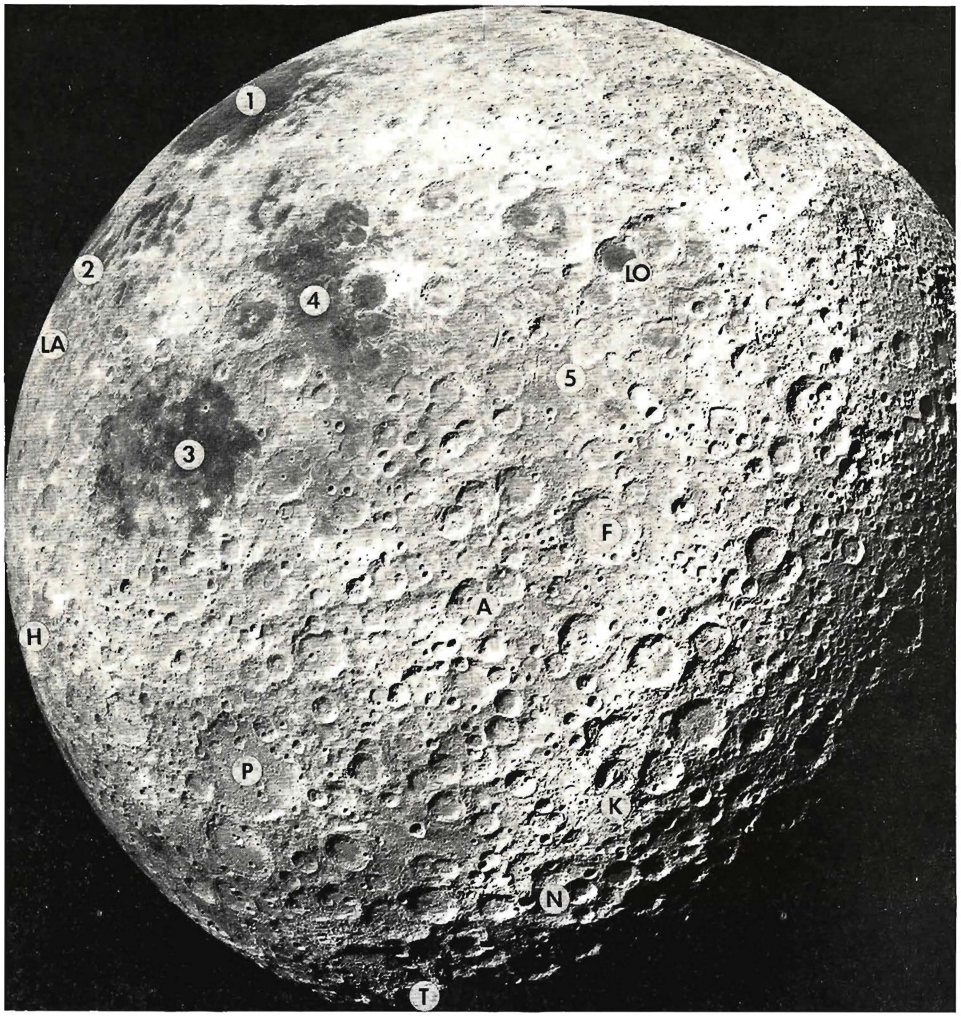

Fig. 2. A photograph of the east side of the moon taken by the Apollo 16 metric camera (3023) after trans-earth injection. The four large and dark patches are mare materials of: (1) Crisium, (2) Fecunditatis, (3) Smythii, and (4) Marginis. Note the bright swirls in and north–northeast of Mare Marginis. Area marked 5 contains the largest concentration of light-colored plains in the region. Large craters discussed in the text are Al-Khwarizmi (A), Fleming (F), Humboldt (H), King (K), Langrenus (LA), Lomonosov (LO), Necho (N), Pasteur (P), and Tsiolkovskij (T).

Geologic Setting

The geology of the region is controlled by multiringed circular impact basins and their ejecta. Two types of terrain are present, terrae and maria. Impact-basin and crater materials compose most of the terrae. The maria, of volcanic origin, are concentrated in basins and their peripheral troughs.

On the geologic map of the east side of the moon (Wilhelms and El-Baz, 1976), units are defined, grouped, and interpreted essentially as on the map of the near side by Wilhelms and McCauley (1971). A major departure however, is the introduction of the Nectarian System. Materials deposited before the formation of the Imbrium Basin, called pre-Imbrian on the nearside map and on other previous lunar geologic maps, are here divided into the Nectarian System and the informal pre-Nectarian (Stuart-Alexander and Wilhelms, 1975). In the southwest part of the map region, ejecta, sculpture, and secondary crater chains of the Nectaris Basin are obvious and make a clear stratigraphic horizon. Materials of the Nectaris Basin and those stratigraphically above them, but older than materials of the Imbrium Basin, are classed as Nectarian. Materials older than the Nectaris Basin are grouped as pre-Nectarian.

Relatively young lunar basins usually display the following: (1) two or more concentric mountain rings, (2) hilly material between the inner rings, (3) a hummocky to lineated ejecta blanket beyond the outermost conspicuous ring, and (4) clustered secondary craters and crater chains in and beyond the lineated ejecta blanket (Baldwin, 1963; Stuart-Alexander and Howard, 1970; Wilhelms, 1970; Hartmann and Wood, 1971; Wilhelms and McCauley, 1971; Howard *et al.*, 1974; Moore *et al.*, 1974; El-Baz, 1974). Preservation of these features in the mapped region is to a degree dependent on basin age, size, and later cratering and other modifications.

There are remnants of at least twelve basins in the studied region, in addition to ejecta from Nectaris and probably Serenitatis (Fig. 3). Two of these basins, the Lomonosov/Fleming and Tsiolkovskij/Stark, are first named here. The names are assigned after major craters that are superposed on the two basins. The basin previously named Al-Khwarizmi (El-Baz, 1973), is here renamed Al-Khwarizmi/King following the same scheme: the craters Al-Khwarizmi (7°N, 107°E) and King (5°N, 120°E) are superposed on the outer of two mapped rings.

Geologic history

After a period of crustal formation about which little is known, the geologic history of the region began with the formation of basins and craters and their overlapping deposits. All the early pre-Nectarian craters and three basins (Tsiolkovskij/Stark, Al-Khwarizmi/King, and Lomonosov/Fleming) are expressed only as subdued rings. Six other basins, (Australe, Fecunditatis, Marginis, Smythii, Serenitatis, and Crisium) are large enough or young enough to retain rugged rims and/or leave traces of ejecta as a mantle on the surrounding terrain.

The formation of the Nectaris Basin west of the studied region initiated the Nectarian Period. Ejecta from Nectaris blanketed older craters and basin materials in the southwestern part of the region. A similar impact created the Humboldtianum Basin north of the region, and smaller impacts formed three other basins (Moscoviense, Milne, and Mendeleev) and numerous craters. Like the Nectarian Period, the succeeding Imbrian Period began with a basin-forming

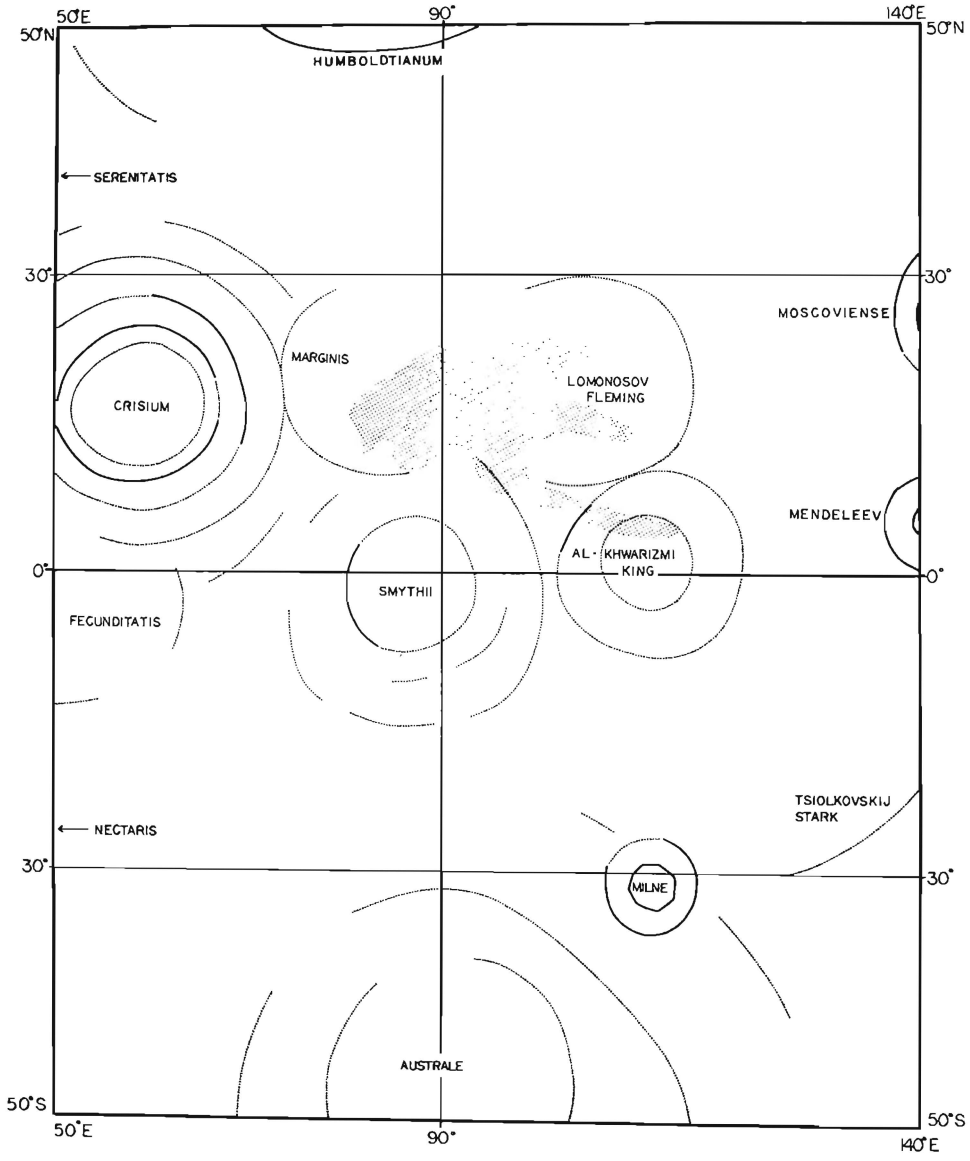

Fig. 3. Basin rings on the east side region of the moon. Solid lines indicate conspicuous arcs and dotted lines indicate subdued segments. The stippled area centered at about 15°N latitude shows light-colored swirls in and north–northeast of Marginis. These sinuous markings have been attributed to seismic shaking antipodal to the Orientale Basin (El-Baz, 1971, 1972a). Grooved and hilly terrain in the same region has also been interpreted to be due to seismically induced modifications (Schultz and Gault, 1975) or to secondary impact of Orientale ejecta (Moore *et al.*, 1974).

impact west of the mapped region. Traces of the Imbrium impact may be present in this region as plains and/or secondary crater clusters.

Later in the Imbrian Period and probably about the time of formation of the Orientale Basin, volcanism resulted in the deposition of mare materials. This early volcanism was followed by more extensive basaltic volcanism in the same and other basins, as well as in a few Imbrian-age craters. During the time of Imbrian volcanism, the frequency of meteorite impacts decreased drastically and continued at a lower rate during the Eratosthenian and Copernican Periods up to the present, resulting in a few craters and minor transport and mixing of the surface materials.

Geologic provinces

A geologic province is an area in which a geologic unit or groups of units related in age and origin are concentrated (McCauley and Wilhelms, 1971). We have mapped eight geologic provinces in the east side region of the moon. The province map (Fig. 4) is more suitable than a detailed geologic map for correlation with data of orbital geophysical and geochemical sensors, because the resolution of these sensors is relatively limited. Refined correlations with individual geologic units are possible only in a few cases at the present stage of data analysis.

The mapped geologic provinces are as follows (see Fig. 4):

1. *Cratered terra.* This province is mostly on the far side and consists of densely packed craters. It contains little basin materials except for the ancient, subdued rings of the Al-Khwarizmi/King, Tsiolkovskij/Stark and Lomonosov/Fleming basins, and a few additional short arcs of rings. The province owes its preservation to a lack of significant modification by relatively young basins, and its materials are the most primitive in the studied region.

2. *Basin rims.* Topographically the most rugged, this province includes the multiple rings and some peripheral terrain of several basins. It is most extensive around the Crisium, Marginis, and Smythii basins.

3. *Mantled terra.* This province includes extensive tracts of terra that appear mantled near young and old basins. Although the distinctive lineated textures usually associated with basin ejecta have not been observed in this province, its proximity to basins suggests that it is composed mostly of degraded basin ejecta.

4. *Lineated ejecta.* The five Nectarian basins are surrounded by blankets of radially lineated ejecta and clusters of secondary impact craters. These features are diagnostic of the impact origin of the source basins, and are most extensive around the Humboldtianum and Nectaris basins.

5. *Old plains.* This province includes densely cratered light-colored plains in topographically low areas. Although most plains may be of impact origin, some may be of volcanic origin.

6. *Young plains.* The province includes light-colored plains that are less densely cratered than old plains, and fills lows near basins and within large craters. Most occurrences are probably derived from impact melts; however, a volcanic

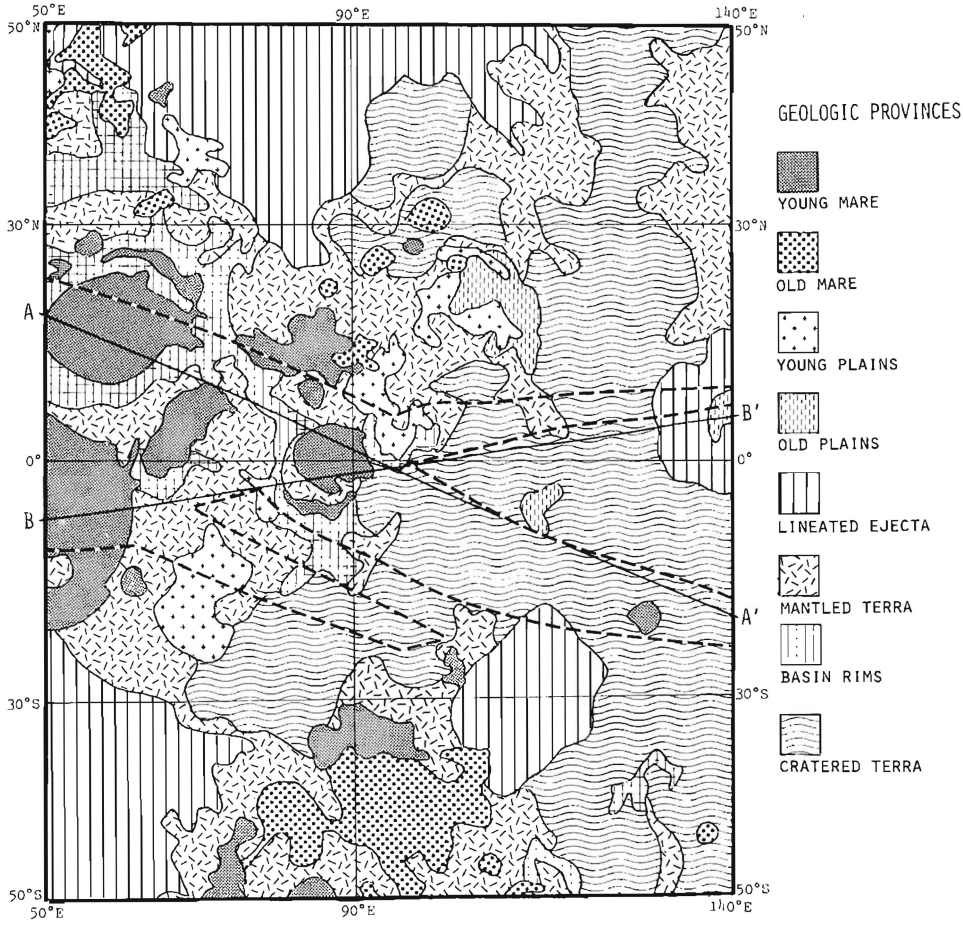

Fig. 4. Geologic provinces on the east side of the moon; based on a detailed geologic map of the same region by Wilhelms and El-Baz (1976). Lines AA′ and BB′ represent the tracks of laser altimeter measurements on Apollo 15 and 16 missions, respectively (see Fig. 5). Dashed lines indicate the boundaries of areas covered by the X-ray fluorescence spectrometers flown on both Apollo 15 and 16 (see Figs. 7a,b).

origin cannot be excluded for all occurrences (e.g. in the Lomonosov/Fleming Basin).

7. *Old mare.* The largest expanse of relatively old mare province is in the Australe Basin. In this locality the mare is overlapped by materials of the Imbrian-age craters Humboldt (27°S, 81°E) and Jenner (42°S, 96°E). This relation indicates that this province includes units that are older than most or all nearside mare materials.

8. *Young mare.* The young mare units are concentrated mainly in the Crisium, Fecunditatis, and Smythii basins and the troughs between them. The crater

Tsiolkovskij in the southeastern part of the region (20°S, 129°E) and a few other craters and depressions on the far side within larger basins contain maria. A conspicuous farside patch of young mare materials not near either a basin or a large crater is centered at 27°S, 130°E (see El-Baz, 1972b, p. 48–49). Data returned from lunar surface missions, including Luna 16 in the map region (0°42′S, 58°18′E), have shown that the mare materials are volcanic basalts.

GEOPHYSICAL AND GEOCHEMICAL DATA

Laser altimeter data

Details of lunar topographic relief were provided by laser altimeter measurements made on Apollo missions 15, 16, and 17. The altimeter, which was part of the metric camera system, measured precise altitudes of the orbiting Command/Service Module above the surface (Wollenhaupt and Sjogren, 1972). Measurements were made at 1.0–1.5° intervals, or every 30–45 km on the surface. Agreements between measurements on the three missions over Mare Smythii region emphasize the accuracy of the profiles.

From laser altimetry and additional data, Kaula *et al.* (1973) have determined a 2–3-km offset toward the earth of the moon's center of mass from its center of figure. This is ascribed to a variable thickness of a low-density terra crust, thinner on the near side than on the far side. It is believed that the maria are concentrated on the near side because the basaltic melts could more easily penetrate the thinner crust. Similarly, local thinning of the crust by basins, and particularly by craters superposed on basins, may explain mare occurrences on the far side.

We have used laser altimeter measurements to construct cross sections in the mapped region (Fig. 5). The measured altitude values were first plotted on a map. Continuous profiles were then drawn using stereoscopic metric camera photographs to interpret the terrain between successive altitude measurements.

Two profiles based on measurements from Apollo 15 and 16 laser altimeters (AA′ and BB′ in Fig. 5) confirm that the near side in the map area averages about 3 km lower in elevation than the far side. This sharp change in elevation occurs just east of 90°E longitude. The higher farside terrain along the profile lines coincides with the cratered terra province (Fig. 4). The nearside terrain traversed by the two profiles is composed mostly of basin-related terra and mare provinces.

The farside part of the Apollo 15 laser altimeter traverse (AA′ in Figs. 4 and 5) crossed terrain that is affected by two old basins: Tsiolkovskij/Stark (between 120°E and 140°E) and Al-Khwarizmi/King (between 100°E and 120°E). On the nearside part, the same traverse crosses terrain that is modified by the Smythii and Crisium basins (see also Fig. 3). The small patch of young mare crossed by this traverse at about 73°E is at least 3 km higher in elevation than the average of the mare surfaces of both Smythii and Crisium, showing that maria do not attain a universal hydrostatic level.

On the farside part of the Apollo 16 traverse (BB′ in Figs. 4 and 5), the lowest segment (between 135°E and 140°E) is represented by the old light-colored plains

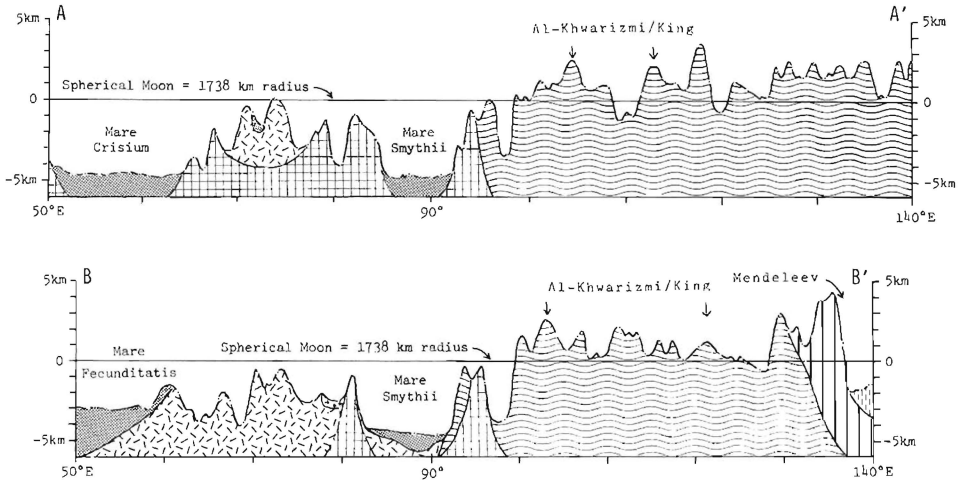

Fig. 5. Schematic cross sections in the studied region. Surface profiles are based on laser altimeter measurements on Apollo 15 (AA') and Apollo 16 (BB'). See Fig. 4 for description of geologic provinces.

that fill the Mendeleev Basin. Between 100°E and 120°E the profile shows a cross section of the Al-Khwarizmi/King Basin, whose surface is 1–2 km higher than the mean lunar spherical radius. The part of the Smythii Basin that is crossed by this altimeter traverse is composed mostly of patches of young mare superposed on hilly terra units. The surface of Mare Fecunditatis (between 50°E and 60°E) is higher by 1–2 km than the fill of both Smythii and Crisium. The high peak centered at about 60°E is due to traversing the rim of the crater Langrenus (9°S, 61°E), which is included in the young mare province.

Lunar sounder data

Another method of generating elevation profiles was provided by the lunar sounder (Phillips *et al.*, 1973). The sounder that was carried on Apollo 17 consisted of a three-frequency coherent radar—5, 15, and 150 MHz. Continuous surface profiles that were optically recorded during the mission show some details of the studied region.

Very high-frequency (VHF) imagery of the Crisium Basin, for example, displays detailed profiles of the mountain chains that ring it (basin rim province) as well as of the mare fill (young mare province). Ward *et al.* (1973) and El-Baz (1975) show that the images of Mare Crisium display both the outer and inner parts of the mare fill, which are separated by a system of wrinkle ridges (Wilhelms, 1973), are characterized by very smooth surface topography. As will be discussed below, the inner part of the basin fill corresponds with the boundaries of the positive gravity anomaly of Crisium.

The high-frequency (HF) images confirm that the roughest surface topography

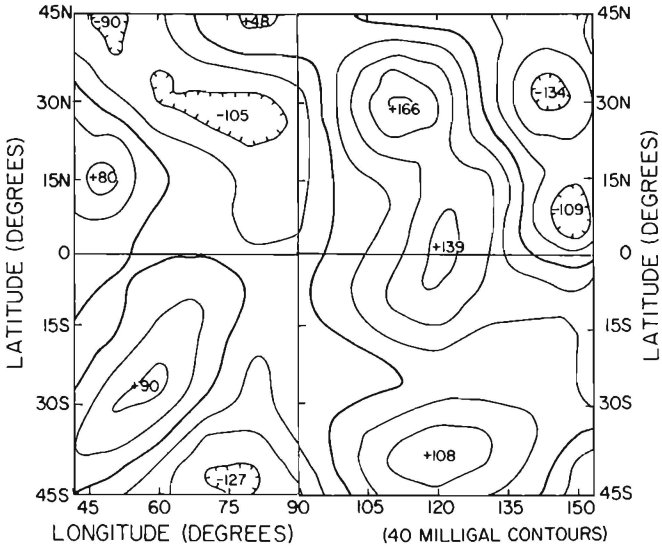

Fig. 6. Map of the lunar farside gravity showing contours of radial accelerations of orbiting satellites at 100-km altitude (Ferrari, 1975).

is in the cratered terra province in the map region. For example, Phillips *et al.* (1973, Fig. 10, p. 2829) discuss details of rough topography of the old and subdued pre-Nectarian craters such as the one centered at 3°S, 125°E (El-Baz, 1972c), southeast of the main ring of Al-Khwarizmi/King Basin.

Gravity data

From laser altimeter and radar sounder profiles as well as other data, it is clear that the impacts that formed the lunar multiringed circular basins resulted in an enormous loss of mass from the impact sites. As a result some of these basins display negative gravity anomalies, whereas others (those filled with mare material) display large positive gravity anomalies or mascons (Muller and Sjogren, 1968).

Detailed gravity measurements, which were made only on the nearside and limb regions, indicate positive gravity anomalies in excess of 200 milligals in Mare Crisium (Sjogren *et al.*, 1972) and Mare Smythii (Sjogren *et al.*, 1974). The mascon of Mare Crisium is bordered by the wrinkle ridge system mentioned above. The mascon of Mare Smythii is displaced toward the northern part of the basin, corresponding with the young mare province (Fig. 4). Therefore, both mascons are located where photogeologic data suggest a probably thick inner fill of circular impact basins. The relatively thin mare in basin troughs and other lowlands, e.g. around the Smythii Basin, does not show mascons.

Gravity data on the studied region also show negative anomalies in ten craters 100 km in diameter or larger (*Geochem. Cosmochim. Acta*, Suppl. 4, V. 1, p. IV).

These negative gravity anomalies are interpreted as a result of the uncompensated loss of mass due to the impacts that created the craters.

More recently, an attempt was made to construct a global gravity map of the moon based on the long-term perturbation in the orbits of both Lunar Orbiter V and the Apollo subsatellites (Ferrari, 1975). The radial acceleration contour map at 100-km altitude for the lunar far side by Ferrari (Fig. 6) shows two negative anomalies and three positive ones in the mapped region. These do not coincide exactly with important mapped features, but Ferrari (personal communication) has indicated to us that the process of data reduction may result in displacements of anomalies by at least five lunar degrees. He also indicated that these data are inaccurate near 90°E and 90°W and higher latitudes than 30°N and 30°S.

The two negative gravity anomalies are located in the vicinity of the Mendeleev and Moscoviense basins on the east edge of the studied region (Figs. 3 and 6). Mendeleev is filled with old light-plains material and no mare material; Moscoviense has some light plains and some thin mare outside the mapped region.

The largest positive anomaly is near the Lomonosov/Fleming Basin, which contains both mare fill and young light-colored plains that could be of volcanic origin.

The second, relatively small positive gravity anomaly lies near the Al-Khwarizmi/King Basin (Fig. 6; see also Fig. 3). This basin is not filled with mare material and lies predominantly in the cratered terra province, although its northern and southern parts contain some old plains. Possible explanations for this poorly understood positive gravity anomaly include: (1) the high topographic elevation of the Al-Khwarizmi/King Basin; even the floor is higher than the mean spherical radius of the moon (Fig. 5); (2) the presence of an elevated region in the basin's center which has been interpreted as the result of dynamic rebound during the basin-forming impact (El-Baz, 1973), a rebound which would uplift the denser materials from the lunar mantle (but this would be expected in all other basins); (3) an anomalous high density of the rocks in this area; and (4) imperfections in the data.

The smallest of the positive gravity anomalies is located east of the Australe Basin (Figs. 3 and 6). One would expect the mascon to lie within the Australe Basin due to the presence of much mare fill (Fig. 4). The eastward displacement of this positive anomaly by 20° is not yet understood. However, other major maria on the limb such as Crisium (and Orientale) do not show mascons in Ferrari's data. As stated above his data is inaccurate near the lunar limbs, particularly farther north and south than 30° latitude.

X-ray fluorescence data

X-ray fluorescence spectrometers were carried in orbit on Apollo missions 15 and 16 to extend geochemical findings to larger areas of the moon from the small spots sampled or analyzed by Surveyor, Apollo, and Luna missions (Adler *et al.*, 1972, 1973).

The X-ray results, reported as concentration ratios of aluminum or magnesium to silicon, correlate fairly well with photogeologic data. Comparisons can be drawn between these ratios and those obtained from analyses of returned rock and soil samples (Adler *et al.*, 1972, 1973). Concentration ratios typical of basaltic mare rocks and anorthositic terra rocks are observed. Ratios of Al:Si (Fig. 7a) and Mg:Si (Fig. 7b) are, in general, inversely related. Extreme values of the ratios are obtained over relatively uninterrupted geologic units—low-Al:Si and high-Mg:Si over maria and the converse over highlands.

This inverse relation (low-Al:Si and high-Mg:Si ratios) holds over Fecunditatis, Crisium, and Smythii with two exceptions: (1) Smythii has a higher Al:Si

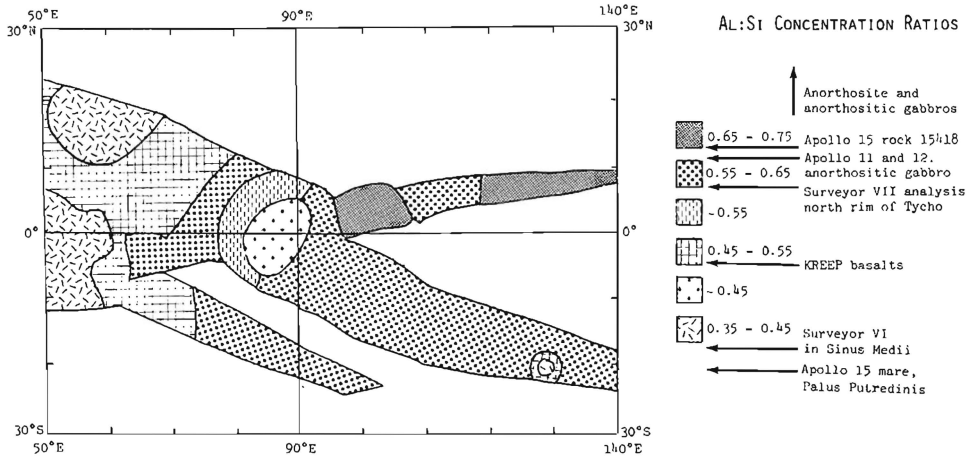

Fig. 7a. Al:Si concentration ratios measured by the Apollo 15 and 16 orbiting X-ray fluorescence spectrometers (Adler *et al.*, 1973). Rock analyses are shown for comparison (Adler *et al.*, 1972, p. 2165).

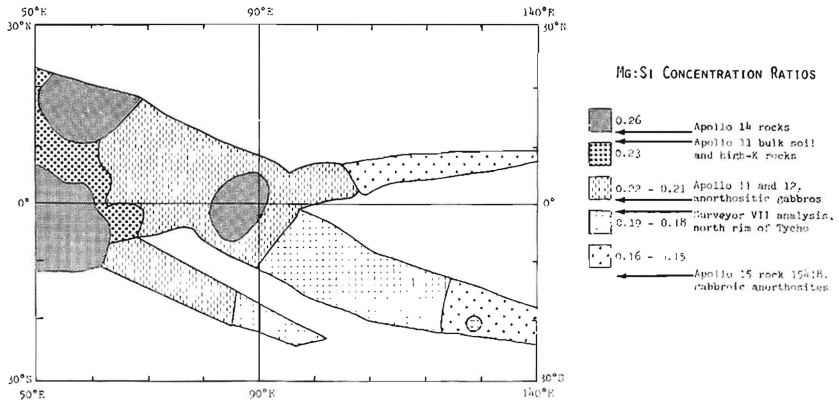

Fig. 7b. Mg:Si concentration ratios measured by the Apollo 15 and 16 orbiting X-ray fluorescence spectrometers. See Figs. 4 and 7a for comparison.

ratio than the other two maria (Fig. 7a), which may be due to the presence of mixed patches of mantled terra and young mare provinces in the southern part of Mare Smythii (Fig. 4); and (2) the high-Mg : Si ratio of Fecunditatis extends farther east than the low-Al : Si ratio (Fig. 7b) over an area of Langrenus ejecta that probably contains fragments of mare rock (see also Fig. 5). The mare-free cratered terra province has the two lowest Mg : Si ratios and the two highest Al : Si ratios; the latter also extend west of this province. Departures from exact inverse correlation may result from instrumental factors, particularly in concentration ratios of Mg : Si (Adler, personal communication).

Intermediate values of the two-element ratios may result from mixtures of mare and terra end-members caused by lunar processes or by limited instrumental resolution. Zones of intermediate values occur on the borders of large maria or correlate with regions in the central and western parts of the map area where small patches of mare and terra are intermixed. Impact cratering has probably mixed mare and terra materials in the regolith of such zones. Also, at a ground resolution of 60 km^2 the instrument integrates values of different units. An alternate possibility for some intermediate values, which remains to be tested by additional data reduction and orbital missions, is the presence of geochemical provinces in the terrae that do not correspond with geologic units or provinces recognized so far.

Gamma-ray data

Gamma-ray spectrometers were flown in orbit with the X-ray fluorescence spectrometers on Apollo 15 and 16 missions. Gamma-ray spectrometry (Fig. 7c) indicates that most of the map area is relatively low in natural radioactivity (Metzger *et al.*, 1973). Most of the overflown areas show natural radioactivity that corresponds to less than one part per million of thorium. The highest, but still moderate, readings of a few parts per million of thorium, are over the maria and the plains east of Langrenus. The latter case agrees with the correlation discussed above between mapped geologic provinces (Figs. 4 and 5) and the geochemical provinces indicated in the X-ray fluorescence data (Figs. 7a,b). Therefore, photogeologic, X-ray fluorescence, and gamma-ray data all show that part of the Langrenus ejecta is composed of mare material.

Far ultraviolet albedo data

The far ultraviolet albedo of the moon (1200–1650-Å range) was measured on Apollo 17 by a spectrometer in the Command/Service Module with a resolution of 30 km or one square degree on the surface (Lucke *et al.*, 1975).

The spectrometer indicated that in the far ultraviolet the moon's geometric albedo is substantially higher than previously thought. This appears to be amply confirmed by results of laboratory measurements of the reflectance of lunar dust samples (Lucke *et al.*, 1975).

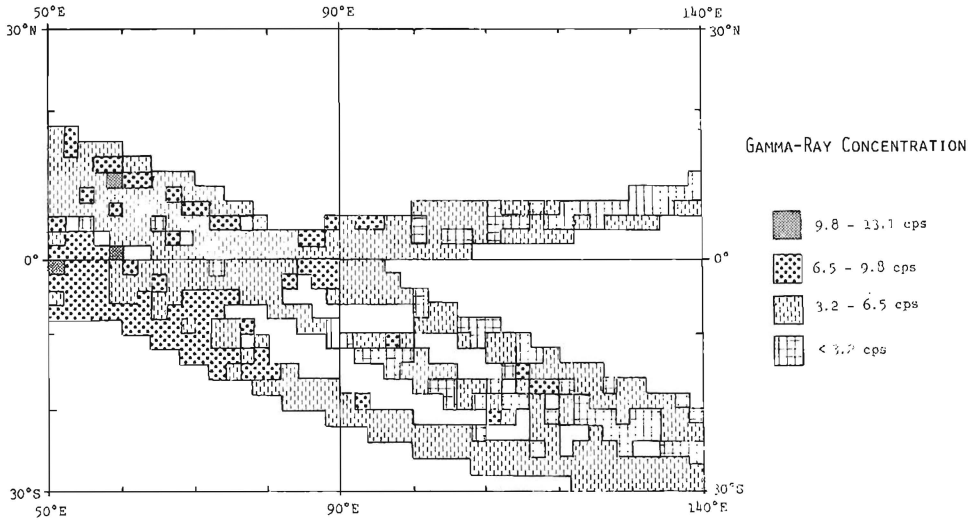

Fig. 7c. Natural gamma-ray emissions measured by the Apollo 15 and 16 orbiting gamma-ray spectrometers (Metzger *et al.*, 1973). Units on the right are counts per second; the lowest correspond to less than one part per million of thorium, and the highest to a few parts per million of thorium.

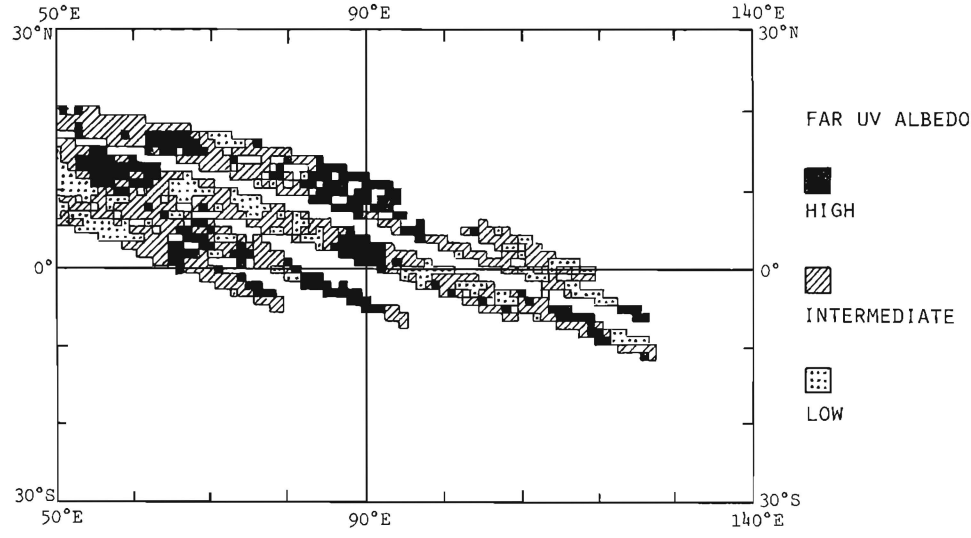

Fig. 7d. Far ultraviolet albedo measurements made on Apollo 17 mission (Lucke *et al.*, 1975; see also *Geochim. Cosmochim. Acta.* Suppl. 5, plate 9). The data are shown in one degree resolution elements. Average geometric albedo of the moon at 1470-Å wavelength is about 4%. Variations in the range ±2.5% are intermediate, greater than +2.5% are high, and less than −2.5% are low.

Unlike the appearance of the moon in visible light, the far ultraviolet albedo shows mare areas to be brighter than the terrae. In the mapped region (Fig. 7d), the highest ultraviolet albedo values are mostly over the dark patches of young mare province in Smythii, Marginis, and Crisium. The largest concentration of the lowest values is obtained over the basin rim province (mostly surrounding Crisium; Fig. 4). Intermediate values do not appear to correspond with any particular geologic or geochemical provinces, although future study may reveal better correlations.

Magnetic data

Apollo 15 subsatellite magnetometer data (Russell *et al.*, 1973) indicate that the lunar field over most of the map area exhibits an average radial component in the range of 0.4 to -0.4 γ. Higher readings (0.8 to 0.4-γ) lie within and east of the crater Humboldt (27°S, 81°E). Two lower values (-0.4 to -0.8 γ) are southeast of Tsiolkovskij: in the crater Subbotin (29°S, 135°E) and northeast of it. All of these variations are in the cratered terra province. They are not yet understood.

Summary and Conclusions

The geology of the studied region on the east limb of the moon is controlled by multiringed circular impact basins and their ejecta. The basins in or near this region are assigned relative ages based on morphologic freshness, density of superposed craters, and presence or absence of surrounding mantled terra deposits. These criteria suggest the following order from oldest to youngest: *pre-Nectarian basins*, Tsiolkovskij/Stark, Al-Khwarizmi/King, Lomonosov/Fleming, Australe, Fecunditatis, Marginis, (or Marginis, Fecunditatis), Smythii, Serenitatis, and Crisium; and *Nectarian basins*, Nectaris, Humboldtianum, Moscoviense, Milne, and Mendeleev.

Correlations are attempted between Apollo orbital data and geologic map provinces in the region that were derived by studying orbital photographs. The maria, which are more abundant of the western (nearside) part of the region than on the eastern (farside) part, are grouped into two provinces, young and old. Two provinces of light-colored plains, also classed as young and old, may be derived from basins and craters (impact origin), although some light plains may be of volcanic origin. At least three of four terra provinces consist mainly of basin materials: radially lineated basin ejecta; the more rugged basin rings and peripheral terrain; and tracts of terra that appear to be mantled. A province consisting of densely packed craters occurs mostly on the farside part of the map area. This province owes its preservation to lack of significant modification by young basins, and contains the most primitive materials in the studied region.

Correlations of photogeologic, geochemical, and geophysical data indicate that the cratered terra province shows the following:

(1) The highest average elevation (above mean lunar radius). This is probably due to the lack of deep penetration by young basins.

(2) The roughest radar sounder profile. This agrees with the observed high density of craters.

(3) The least gravity field variations. This again is probably due to the lack of deep young basins that show positive or negative anomalies depending on whether or not they are deeply filled with mare materials.

(4) The highest Al:Si and lowest Mg:Si concentration ratios. Based on the findings of the lunar surface missions, this suggests an anorthositic composition of rocks in the province.

(5) The lowest gamma-ray concentrations. This probably is due to the lack of mare materials and KREEP basalts in the province.

(6) The only variations in the radial component of the magnetic field in the studied region.

Data on the young mare province, which includes the youngest volcanic materials show:

(1) The lowest average elevation in the region (below mean lunar radius). This province includes mare fill of deep circular basins.

(2) The smoothest radar sounder profile. This agrees with observed photogeologic characteristics and the interpretation of the mare material as basaltic flows of volcanic origin.

(3) The largest gravity anomalies or mascons (particularly in Crisium and Smythii). The great thickness of the dense basaltic rocks may be responsible for these mascons.

(4) The lowest Al:Si and highest Mg:Si concentration ratios. Compositions implied by these values support the interpretation that mare materials are basalts.

(5) The highest, but still moderate, gamma-ray concentrations of a few parts per million of thorium. This agrees with readings over the eastern maria on the near side of the moon.

(6) The highest ultraviolet albedo. This may be related to the fact that this province displays the lowest optical albedo.

On a local level, correlation of photogeological and Apollo orbital data may also be significant. As stated above, for example, high-Al:Si concentration ratios are obtained where Mg:Si ratios are low and vice versa. The inverse relation (low-Al:Si and high-Mg:Si ratio) holds over the Maria Fecunditatis, Crisium, and Smythii, except that: (a) Smythii has a higher Al:Si ratio, which is interpreted to be due to the presence of mantled terra units; and (b) the high-Mg:Si ratio characteristic of Mare Fecunditatis extends farther east than the limits of the low-Al:Si ratio. This supports the interpretation that Langrenus ejecta is composed in this area of mare materials. The gamma-ray concentrations over the same area are as high as they are over Mare Fecunditatis.

It is concluded that correlations of photogeologic data with geochemical and geophysical data help to better understand features portrayed in lunar photo-

graphs. Correlations are necessary for the extrapolation of groundtruth data from rock and soil sampling sites to larger areas of the moon. It is anticipated that more detailed correlations with sensor data at finer resolution will further our knowledge of lunar surface features, particularly those in the relatively complex terrae.

Acknowledgments—The authors wish to acknowledge the benefits gained from discussions with Apollo orbital experiment principal investigator groups during formal and informal gatherings. The detailed geologic map upon which this study is based was prepared on behalf of NASA under contract number W-13,130. This study was performed under NASA experiment S-222. The authors are indebted to B. K. Lucchitta, H. J. Moore, and J. W. Head for reviewing this paper.

References

Adler I., Gerard J., Trombka J., Schmadebeck R., Lowman P., Blodget H., Yin L., Eller E., Lamothe R., Gorenstein P., Bjorkholm P., Harris B., and Gursky H. (1972) The Apollo 15 X-ray fluorescence experiment. *Proc. Lunar Sci. Conf. 3rd*, p. 2157–2178.

Adler I., Trombka J. I., Schmadebeck R., Lowman P., Blodget H., Yin L., Eller E., Podwysocki M., Weidner J. R., Bickel A. L., Lum R. K. L., Gerard J., Gorenstein P., Bjorkholm P., and Harris B. (1973) Results of the Apollo 15 and Apollo 16 X-ray experiment. *Proc. Lunar Sci. Conf. 4th*, p. 2783–2791.

Baldwin R. B. (1963) *The Measure of the Moon.* University of Chicago Press, Chicago, Ill. 488 pp.

El-Baz F. (1971) Light colored swirls in the lunar maria (abstract). *EOS (Trans. Amer. Geophys. Union)* **52**, 856.

El-Baz F. (1972a) The Alhazen to Abul Wafa swirl belt: An extensive field of light-colored, sinuous markings. In *Apollo 16 Preliminary Sci. Report*, NASA publication SP-315, p. 29-93 to 29-97.

El-Baz F. (1972b) New geological findings in Apollo 15 lunar orbital photography. *Proc. Lunar Sci. Conf. 3rd*, p. 39–61.

El-Baz F. (1972c) Discovery of two lunar features. In *Apollo 16 Preliminary Sci. Report*, NASA publication SP-315, p. 29-33 to 29-38.

El-Baz F. (1973) Al-Khwarizmi: A new-found basin on the lunar far side. *Science* **180**, 1173–1176.

El-Baz F. (1974) Surface geology of the moon. *Ann. Rev. Astronom. Astrophys.* **12**, 135–165.

El-Baz F. (1975) The moon after Apollo. *Icarus* **25**. In press.

Ferrari A. J. (1975) A comparison of near and farside lunar gravity (abstract). In *Lunar Science VI*, p. 260–262. The Lunar Science Institute, Houston.

Hartmann W. K. and Wood C. A. (1971) Moon: Origin and evolution of multi-ringed basins. *The Moon* **3**, 4–78.

Howard K. A., Wilhelms D. E., and Scott D. H. (1974) Lunar basin formation and highland stratigraphy. *Revs. Geophys. Space Phys.* **12**, 309–327.

Kaula W. M., Schubert G., Lingenfelter R. E., Sjogren W. L., and Wollenhaupt W. R. (1973) Lunar topography from Apollo 15 and 16 laser altimetry. *Proc. Lunar Sci. Conf. 4th*, p. 2811–2819.

Lucke R. L., Henry R. C., and Fastie W. G. (1975) Far ultraviolet albedo of the moon from Apollo 17 (abstract). In *Lunar Science VI*, p. 528–530. The Lunar Science Institute, Houston.

McCauley J. F. and Wilhelms D. E. (1971) Geological provinces of the near side of the moon. *Icarus* **15**, 363–367.

Metzger A. E., Trombka J. I., Peterson L. E., Reedy R. C., and Arnold J. R. (1973) Lunar surface radioactivity. Preliminary results of the Apollo 15 and Apollo 16 gamma-ray spectrometer experiments. *Science* **179**, 800–803.

Moore H. J., Hodges C. A., and Scott D. H. (1974) Multi-ringed basins—illustrated by Orientale and associated features. *Proc. Lunar Sci. Conf. 5th*, p. 71–100.

Muller P. M. and Sjogren W. L. (1968) Mascons: Lunar mass concentrations. *Science* **161**, 680–684.

Phillips R. J., Adams G. F., Brown W. E., Eggleton R. E., Jackson P., Jordon R., Peeples W. J., Porcello L. J., Ryu J., Schaber G., Sill W. R., Thompson T. W., Ward S. H., and Zelenka J. S. (1973) The Apollo 17 lunar sounder. *Proc. Lunar Sci. Conf. 4th*, p. 2821–2831.

Rükl A. (1972) *Maps of Lunar Hemispheres.* D. Reidel, Dordrecht-Holland. 24 pp. + 6 maps.

Russell C. T., Colemann P. J., Lichtenstein B. R., Schubert G., and Sharp L. R. (1973) Subsatellite measurements of the lunar magnetic field. *Proc. Lunar Sci. Conf. 4th*, p. 2833–2845.

Schultz P. H. and Gault D. E. (1975) Seismically induced modification of lunar surface features (abstract). In *Lunar Science VI*, p. 724–726. The Lunar Science Institute, Houston.

Sjogren W. L., Gottlieb P., Muller P. M., and Wollenhaupt W. R. (1972) S-Band transponder experiment. In *Apollo 15 Preliminary Sci. Report*, NASA publication SP-289, p. 20-1 to 20-6.

Sjogren W. L., Wollenhaupt W. R., and Wimberly R. N. (1974) Lunar gravity via the Apollo 15 and 16 subsatellites. *The Moon* **9**, 115–128.

Stuart-Alexander D. E. and Howard K. A. (1970) Lunar maria and circular basins—A review. *Icarus* **12**, 440–456.

Stuart-Alexander D. E. and Wilhelms D. E. (1975) Nectarian System, a new lunar time-stratigraphic unit. *U.S. Geol. Survey J. Res.*, **3**, 53–58.

Ward S. H., El-Baz F., Maxwell T. A., Peeples W. J., and Sill W. R. (1973) Radar descriptions of lunar surface features (abstract). Abstracts with Programs, 1973 Ann. Meet. Geol. Soc. Amer., p. 855.

Wilhelms D. E. (1970) Summary of lunar stratigraphy—telescopic observations. U.S. Geol. Survey Prof. Paper 599-F, 47 pp.

Wilhelms D. E. (1973) Geologic map of the northern Crisium region. In *Apollo 17 Preliminary Sci. Report*, NASA publication SP-330, p. 29-29 to 29-34.

Wilhelms D. E. and El-Baz F. (1976) Geologic map of the east side of the moon. U.S. Geol. Surv. Map I-948. In press.

Wilhelms D. E. and McCauley J. F. (1971) Geologic map of the near side of the moon. U.S. Geol. Surv. Map I-703.

Wollenhaupt W. R. and Sjogren W. L. (1972) Comments on the figure of the moon based on preliminary results from laser altimetry. *The Moon* **4**, 337–347.